Energy conversion in ferrofluids: Magnetic nanoparticles as motors or generators

F. Gazeau,[1] C. Baravian,[2] J.-C. Bacri,[1] R. Perzynski,[1] and M. I. Shliomis[1,3]
[1]*Laboratoire d'Acoustique et d'Optique de la Matière Condensée, URA CNRS, Université de Paris–6, Tour 13, Case 78, 75252 Paris Cedex 05, France*
[2]*Laboratoire de Biorhéologie et Hydrodynamique Physicochimique, URA CNRS, Université de Paris–6 et 7, Tour 33, Case 7056, 75251 Paris Cedex 05, France*
[3]*Department of Physics of Complex Systems, Weizmann Institute of Science, Rehovot 76100, Israel*
(Received 3 February 1997)

We submit a $CoFe_2O_4$ ferrofluid in rigid rotation (and then in a Couette flow) to an alternating magnetic field. Rotational viscosity and transverse magnetization are measured simultaneously. Depending on the relative values of fluid vorticity and field frequency, the magnetic particles behave as nanomotors or nanogenerators. It demonstrates the energy conversion between the magnetic and kinetic degrees of freedom of the particles. The effect of an hydrodynamic shear on the spectrum of relaxation times evidences an intimate structure of the ferrofluid consisting of small chains of dipoles. [S1063-651X(97)03106-1]

PACS number(s): 82.70.Dd, 83.80.Gv, 47.32.−y, 75.50.Mm

Magnetic fluids (MFs) are colloidal solutions of single-domain magnetic nanoparticles. Actually, such dipolar fluids with anisotropic interactions raise up a growing interest. Endeavors to elucidate their internal structure are put forward in numerous theoretical and numerical studies [1–5]. MFs are also attractive because of the interplay between the magnetic and the rotational degrees of freedom of the particles [6,7]. It enriches the picture of hydrodynamic and magnetic phenomena in MF under time-dependent magnetic fields. Internal rotation (particles can rotate relatively to their surrounding fluid) causes spectacular effects such as under a rotating field, entrainment of the MF by the field [6,8,9] or ''starfish instability'' of a MF drop [10]; under an oscillating field, the ''negative viscosity'' phenomenon in a Poiseuille flow [11–13] or the vortico-magnetic resonance [14]. In these experiments, the energy of the time-dependent field is partially transformed into kinetic energy of particles or, conversely, an alternating field is created at the expense of the particle spinning. We present below results clearly establishing this nontrivial mechanism of energy conversion. We measure directly and simultaneously on the same MF sample (submitted to a solid rotation and experiencing an alternating magnetic field) the coefficient of rotational viscosity and the transverse magnetic susceptibility. Our experimental results are clearly understood in the framework of ferrohydrodynamics. We demonstrate that depending on the ratio of the field frequency to the fluid vorticity, ω/Ω, the particles behave as nanomotors or nanogenerators, changing their working regime at the crossover point $\omega=\Omega$. We show that the recent observations in a MF of a ''negative viscosity'' effect [12] and of a vortico-magnetic resonance [14] represent two sides of the same physical phenomenon: they reflect energy conversion between the magnetic and rotational degrees of freedom. We also evidence that such dynamical experiments are powerful tools to study the intimate structure of these dipolar magnetic fluids. A large distribution of relaxation times exist inside the MF, we correlate this distribution to a chaining of the magnetic particles under the conjugated effect of alternating field and mechanical rotation.

We use an ionic MF [15] composed of cobalt Ferrite magnetic particles. The magnetic volume fraction φ, because of a nonmagnetic layer at the particle surface, is about 10% smaller than the one measured by chemical titration of iron. Particle sizes and dipolar interaction parameter are determined in the dilute regime ($\varphi\approx 1\%$) by measurements of initial magnetic susceptibility χ and by small angle neutron scattering (SANS) [16]. The magnetic measurements lead to a magnetic diameter $d_m=13.6$ nm (using saturation magnetization of the cobalt ferrite $M_s=400$ G) to be compared to the SANS size determinations ($d_W=14.1$ nm and $R_g=7.8$ nm). The parameter ϵ of dipolar interaction is equal to

$$\epsilon=\frac{\pi\chi}{\varphi}=\frac{2m_0^2}{d_m^3 k_B T}=5.3,$$

with the particle magnetic moment $m_0=M_s(\pi/6)d_m^3$, k_B being the Boltzman constant, and T the room temperature. The colloidal stability requires a repulsive force in order to counterbalance the van der Waals isotropic attractions and the attractive part of the anisotropic dipolar interaction. This is realized through screened electrostatic repulsion: the particles are also macroions with a negative superficial density of charges. The SANS study as a function of φ on water based suspensions of such particles shows that the repulsive interaction is $\partial[\varphi(\partial\mu/\partial\varphi)]/\partial\varphi\approx 10k_BT$, where μ is the chemical potential of the solution. In the experiment reported below, the particles are dispersed in glycerol with $\varphi=13\%$. The dispersive energy of the particles in glycerol is even lower because its dielectric constant is two times smaller. The initial magnetic susceptibility of the MF equals $4\pi\chi=4.4$. The viscosity of glycerol is $\eta_{\rm gly}=1$ Pa s at 20 °C and Brownian relaxation times of isolated particles are of the order of millisecond. In the absence of an external field, the sample has a Newtonian behavior in the shear rate range $20<\dot{\gamma}<100\ {\rm s}^{-1}$, the relative viscosity of the MF being $\eta/\eta_{\rm gly}=5$.

To probe experimentally the coupling of hydrodynamic and magnetic phenomena, we perform simultaneously rheological and magnetic measurements. A cylindrical Couette

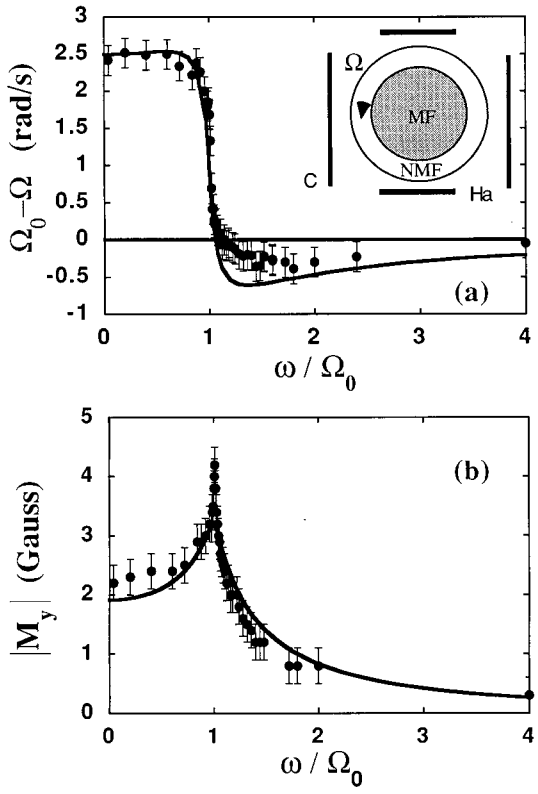

FIG. 1. Rigid rotation of the magnetic fluid. (a) Difference $\Omega_0 - \Omega$ of the angular velocities of the MF cylinder without magnetic field applied ($\Omega_0 = 157$ rad/s) and under magnetic field (Ω) as a function of ω/Ω_0. (b) Modulus of the transverse magnetization $|M_y|$ as a function of ω/Ω_0. The solid lines illustrate the best fit using the chain distribution function (see text): $\tau_0 = 1.6$ ms, $\epsilon = 5$, and $\varphi = 13\%$. Inset: experimental setup for rigid rotation of the MF. C, coils; Ha, Hall-effect transducers.

rheometer is adapted to our experiment (see inset of Fig. 1). The MF fills the inner moving cylinder (with radius $R_1 = 5$ mm) and thus undergoes a rigid rotation around the axis of cylinder (axis z). The outer cylinder ($R_2 = 6$ mm) is motionless. The gap is filled with a Newtonian nonmagnetic fluid (NMF) present only because of technical limitation of the apparatus. The whole system is put between two coils creating the alternating field $H_x = H \cos\omega t$ transverse to the axis of the cylinder. We measure the angular velocity Ω of the MF cylinder (Ω_0 without magnetic field) under a constant applied mechanical torque $\mathcal{M}$. The magnetization M_y in the direction perpendicular to the field is detected with two Hall-effect transducers.

Figures 1(a) and 1(b) show, respectively, the difference of angular velocities $\Omega_0 - \Omega$ and the modulus of M_y as a function of ω/Ω_0. In this experiment, $\Omega_0 = 157$ rad/s and the field amplitude $H = 65$ Oe (taking into account the cylinder demagnetizing factor). As can be seen in Fig. 1(a), the difference $\Omega_0 - \Omega$ is positive for $\omega < 1.2\Omega_0$ expressing the fact that a stationary or a slow oscillating field impedes free rotation of the MF. The nearer ω to Ω_0, the more drastically $\Omega_0 - \Omega$ decreases and becomes negative at $\omega > 1.2\Omega_0$. Thus, for an applied torque $\mathcal{M} = \text{const}$, the MF cylinder actually rotates faster under magnetic field than in zero field. Parallelly, it is apparent in Fig. 1(b) that $|M_y|$ presents a sharp resonance for $\omega = \Omega_0$. Qualitatively, if the field is off, the MF rotates as a whole in a rigid rotation. However, under field, the MF rotation, strictly speaking, ceases to be rigid since the field causes a particle spin relatively to the surrounding fluid. The friction experienced by each particle results in internal stresses, which may be written as $2\eta_r\Omega$, where η_r is the rotational viscosity. If $\omega < \Omega$, the field impedes the free particle rotation ($\eta_r > 0$) and it leads to a certain decrease of Ω. Conversely, if $\omega > \Omega$, the field forces the particles to rotate faster than the fluid. Some part of the ac field energy is transformed into a spinning energy of the particle, which in turn accelerates the MF rotation. This increase of Ω just expresses the negative viscosity effect [11,12]: $\eta_r < 0$. The other side of the problem is that the MF rotation influences its magnetization $\vec{M}$. The particles rotate together with their magnetic moment which determines $\vec{M}$. Consequently, the particle angular velocity (always between ω and Ω) can be considered as the eigenfrequency of rotation of vector $\vec{M}$. Hence, at $\omega = \Omega$, this eigenfrequency coincides with ω, the whole system rotates in a rigid rotation and a vortico-magnetic resonance arises [14]. At the resonance, the vector $\vec{M}$ rotates as a whole, i.e., $M_x^2(t) + M_y^2(t) = \text{const}$, whereas in the quiescent MF ($\Omega = 0$) the only component of magnetization to exist is $M_x(t)$. Thus simple arguments predict simultaneously the change of sign of η_r and the magnetic resonance of M_y at the same frequency $\omega = \Omega$.

Quantitatively, the friction torque $\mathcal{M}$ acting on our MF cylinder can be expressed through the $r\varphi$ component of the symmetric stress tensor [6]

$$\sigma_{r\varphi} = \eta\left(\frac{\partial \nu_\varphi}{\partial r} - \frac{\nu_\varphi}{r}\right) - \frac{1}{2}(M_r H_\varphi - M_\varphi H_r) + \frac{B_r H_\varphi}{4\pi}, \quad (1)$$

where $B_r = H_r + 4\pi M_r$. Writing the second term of Eq. (1) as $(\vec{M}\times\vec{H})_z = -M_y H_x$ and substituting the velocities $\nu_\varphi = \Omega r$ for the MF inside the rotating cylinder and $\tilde{\nu}_\varphi = (\Omega R_1^2)/(R_2^2 - R_1^2)[(R_2^2/r) - r]$ for the NMF in the gap, we find

$$\sigma_{r\varphi} = \frac{M_y H_x}{2} + \frac{B_r H_\varphi}{4\pi}, \quad \tilde{\sigma}_{r\varphi}|_{r=R_1} = -2A\tilde{\eta}\Omega + \frac{\tilde{B}_r \tilde{H}_\varphi}{4\pi}, \quad (2)$$

where the tilde refers to NMF and $A = R_2^2/(R_2^2 - R_1^2)$. Taking into account the boundary conditions for B_r and H_φ on the surface $r = R_1$ of the MF, the torque writes

$$\mathcal{M} = 4\mathcal{V}(\tilde{\eta}A\Omega + \overline{M_y H_x}/4), \quad (3)$$

where $\mathcal{V}$ is the volume of the cylinder and the upper line means averaging over the period of the field variation. In the framework of the linear response—the field is low enough—we may write $M_i = \chi_{ik} H_k$ with $\chi_{ik} = \chi_\parallel \delta_{ik} - (\chi_\perp / \Omega) e_{ikl}\Omega_l$, the tensor of magnetic susceptibility of the moving MF. The tensor components are determined by the evolution equation of the magnetization [6] $d\vec{M}/dt = \vec{\Omega}\times\vec{M} - 1/\tau_B(\vec{M} - \chi\vec{H})$, where τ_B is the Brownian relaxation time of magnetic particles and χ is the static susceptibility of the

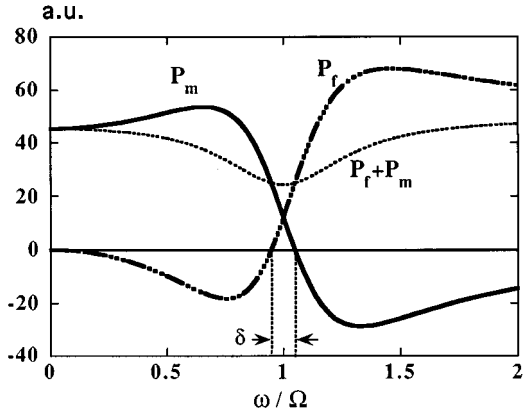

FIG. 2. Energetical description. Power of the motor rotating the cylinder $P_m=(\vec{\mathcal{M}}\cdot\vec{\Omega})$ (solid line), power of the field $P_f=-\mathcal{V}(\overrightarrow{M\cdot H})$ (dashed line), and total power P_m+P_f (dotted line) as a function of ω/Ω. $\delta\Omega=\omega_2-\omega_1$. For these curves, $\Omega\tau_B=3$ (single relaxation time model).

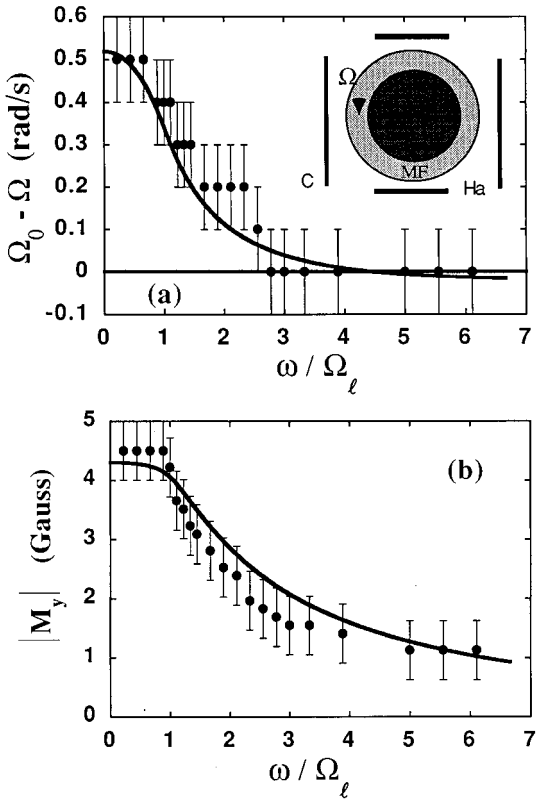

FIG. 3. Couette flow of the magnetic fluid. (a) Difference $\Omega_0-\Omega$ of the angular velocities of the MF cylinder ($\Omega_l=63$ rad/s and $\dot{\gamma}=30\ \mathrm{s}^{-1}$) as a function of ω/Ω_l. (b) Modulus of the transverse magnetization $|M_y|$ as a function of ω/Ω_l. The $(\Omega_0-\Omega)$ signal is weak and the experimental discrete values are connected to the apparatus resolution. The solid lines illustrate the best fit using the chain distribution function: $\tau_0=1.6$ ms, $\tilde{\epsilon}=3.2$, and $\varphi=13\%$. Inset: experimental setup for Couette flow of the MF. C, coils; Ha, Hall-effect transducers.

MF. With $\overline{M_yH_x}=\chi_\perp' H^2/2$, the second term in Eq. (3) takes the form $\eta_r\Omega$ where the rotational viscosity coefficient η_r is

$$\eta_r=\chi_\perp' H^2/8\Omega=(1/8)\chi\tau_B H^2[1+(\Omega^2-\omega^2)\tau_B^2]K^{-2}, \tag{4}$$

with $K^2=[1+(\Omega^2-\omega^2)\tau_B^2]^2+4\omega^2\tau_B^2$. It becomes negative for $\omega^2\tau_B^2>\Omega^2\tau_B^2+1$. Let us compare the powers that the motor and the field spend to rotate and magnetize the magnetic fluid. The field's power is determined by the expression $P_f=-\mathcal{V}(\overrightarrow{M\cdot H})$ and the power of the motor by $P_m=(\vec{\mathcal{M}}\cdot\vec{\Omega})$. It yields

$$P_f=\omega\chi_\parallel'' H^2\mathcal{V}/2=(1/2)\chi H^2\mathcal{V}\omega^2\tau_B[1+(\omega^2-\Omega^2)\tau_B^2]K^{-2},$$

$$P_m=4A\tilde{\eta}\Omega^2\mathcal{V}+(1/2)\chi H^2\mathcal{V}\Omega^2\tau_B[1+(\Omega^2-\omega^2)\tau_B^2]K^{-2}. \tag{5}$$

Figure 2 represents P_f and P_m and the sum P_f+P_m, as a function of the ratio ω/Ω for $\Omega\tau_B=3$. An oscillating field produces a work ($P_f>0$) for the field frequencies $\omega>\omega_1=\Omega\sqrt{1-(\Omega\tau_B)^{-2}}$, while a slow oscillating field is generated at the *expense* of the motor ($P_f<0$) if $\omega<\omega_1$. Conversely, the motor is working ($P_m>0$) at the low field frequency $\omega<\omega_2=\Omega\sqrt{1+(\Omega\tau_B)^{-2}}$ and rotates at the *expense* of the field ($P_m<0$) for $\omega>\omega_2$. Thus particles behave as *nanomotors* for $\omega>\omega_2$ and as *nanogenerators* for $\omega<\omega_1$. The equation $P_f=P_m$ determines the crossover frequency of the field, ω_*. Neglecting the viscosity of NMF in Eq. (5), we find $\omega_*=\Omega$ at the minimum of the sum P_f+P_m.

Experimentally, we measure the modulus $|\chi_\perp|$ and the difference $(\Omega_0-\Omega)$ of the angular velocities at a given torque; this difference is related to the rotational viscosity via $\eta_r=A\tilde{\eta}(\Omega_0-\Omega)/\Omega$. The theoretical dependences of these quantities on the ratio ω/Ω reveal that the larger $\Omega\tau_B$, the sharper is the magnetic resonance [14] and the more steeply falls the rotational viscosity nearby the resonance frequency. Therefore, to describe the sharp-edge resonance maximum, experimentally obtained (see Fig. 1), we have to admit the existence of a sufficiently wide spectrum of relaxation times τ_B, including very long time compared to the Brownian time for an isolated particle of volume V, $\tau_0=3\eta V/k_BT$. We suppose that such a spectrum originates from spatially distributed chains of dipoles aligning nose to tails, each chain behaving independently. Indeed, the pioneer work of de Gennes and Pincus [1] show that the highly anisotropic nature of the interaction between dipolar spheres favors chain formation. Recent numerical simulations taking into account dispersive interactions, report the existence of internal dynamical structures if the isotropic attractive energy in the colloid is below a specific threshold [2–4]. In ferrofluids, apart from SANS studies [17], experimental work to elucidate this stage of structuration—chaining of a few nanoparticles—is lacking. Evidence for anisotropic chaining exist only in analogous systems with microscopic, and thus directly observable, length scale [18,19].

In the present MF, an additional clue supporting the internal structures existence is given by the effect of an hydrodynamic shear. Figure 3 shows the difference of angular velocities $\Omega_0-\Omega$ [Fig. 3(a)] and the modulus of transverse magnetization $|M_y|$ [Fig. 3(b)] as a function of ω/Ω_l, in an

experiment where the MF (see the inset in Fig. 3) fills the gap between the two cylinders (Couette flow of the MF). Thus contrary to the first experiment, where the shear rate $\dot{\gamma}$ is zero (solid rotation), for this Couette flow, $\dot{\gamma}=30\ \mathrm{s}^{-1}$. It corresponds in our geometry to the local vorticity $\Omega_l = 63$ rad/s. It is apparent that the $|M_y|$ sharp resonance and the drastic decrease of rotational viscosity do not exist in the shear flow configuration: it indicates that long relaxation times associated with the most long chains do not exist any more in the system. This change of dynamical behavior under shear may thus be related to a modification of internal structure of the MF.

We analyze those experiments with a statistical model of chains taking into account only dipole-dipole interaction through the parameter ϵ. This energy scale determines both the energy gain due to the particle chain formation and the flexibility of the chains: the value ϵd represents the chain correlation length [1]. The dipole-dipole interaction free energy μ_N^0 per particle in chains of N particles is $\mu_N^0=-[(N-1)/N]k_BT\ \ln[\sinh(\epsilon)/\epsilon]$. Equilibrium thermodynamic requires [20] that X_N, the total volume of chains of N particles by unit volume of MF, writes $X_N=Np^N\epsilon/\sinh(\epsilon)$, with $p=X_1\sinh(\epsilon)/\epsilon$. The global volume fraction φ of particles may be expressed as $\varphi=\Sigma_N X_N=[p/(1-p)^2][\epsilon/\sinh(\epsilon)]$. The probability P_N to have a chain of N particles being $P_N=(X_N/N)/\Sigma_N(X_N/N)$, is completely determined by φ and ϵ. It gives for the mean number of particles in a chain in a zero field, $\langle N\rangle=\Sigma_N NP_N$ and $\langle N\rangle\approx 1$, for $p\ll 1$. In order to average η_r and $|\chi_\perp|$ over the chain distribution, it is necessary to know the contribution χ_N of N-particle chains to the static susceptibility and their Brownian time τ_{BN}. χ_N may be written as $\chi_N=(X_N/NV)(m_0^2/3k_BT)(\langle\vec{r}^2\rangle_N/d_m^2)$, where the end-to-end vector of the chain is given for $\epsilon>1$ by the expression $\langle\vec{r}^2\rangle_N=2N\epsilon d_m^2\{1-[(1-e^{-N/\epsilon})/(N/\epsilon)]\}$ [21]. We propose [22] the following expression for the Brownian time τ_{BN}: $\tau_{BN}=\tau_0(\langle\vec{r}^2\rangle_N/d_m^2)^{3/2}(1+3d_m^2/\langle\vec{r}^2\rangle_N)/4$. The results of averaging η_r and $|\chi_\perp|$ are presented in Figs. 1 and 3 by solid lines together with experimental data. The same averaging parameters fit both η_r and $|\chi_\perp|$. We find $\epsilon=5$, $\tau_0=1.6$ ms, and $\varphi=13\%$ in zero hydrodynamic shear (rigid rotation: Fig. 1). Experimental features such as the sharp resonance and the steep decrease of rotational viscosity associated with an asymmetry of the curves are correctly reproduced. Moreover, the interaction parameter deduced from this experiment $\epsilon=5$, is very close to the above evaluation coming from static magnetic measurements in more dilute solutions ($p<0.2$), $\epsilon=5.3$. For the Couette flow (Fig. 3), we obtain a reduced apparent parameter $\tilde{\epsilon}=3.2$, $\tau_0=1.6$ ms, and $\varphi=13\%$. The distributions of the number N of particles per chain and of the relaxation times, corresponding to the cases of rigid rotation and shear flow, are compared in Fig. 4: without shear, the mean number of particles in a chain is $\langle N\rangle=2.0$ and the mean relaxation time $\langle\tau_{BN}\rangle=5.2\tau_0$; under our experimental shear however, they become $\langle N\rangle=1.36$ and $\langle\tau_{BN}\rangle=1.84\tau_0$. It appears that, in addition to thermal fluctuations which in both cases of rigid rotation and shear flow limit the chain formation, the shear induces fracture of the chains. It thus leads to a reduced interaction parameter

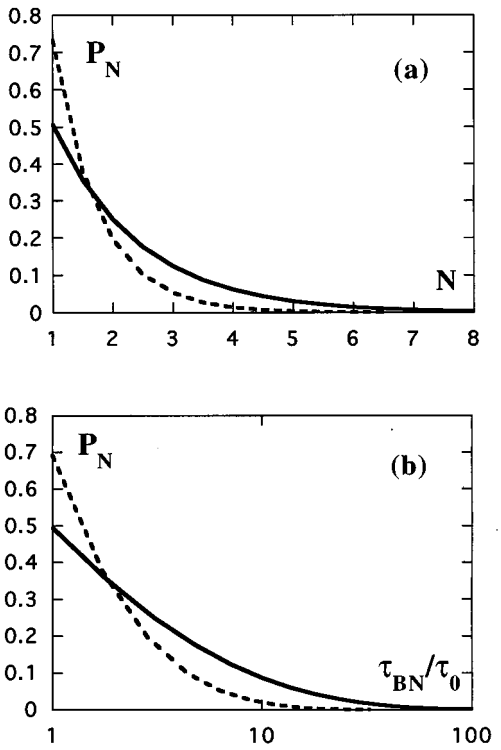

FIG. 4. (a) Distribution P_N of the number N of particles per chain. (b) Relaxation time distribution. Solid lines: $\tau_0=1.6$ ms, $\epsilon=5$, and $\varphi=13\%$ (rigid rotation). Dashed lines: $\tau_0=1.6$ ms, $\tilde{\epsilon}=3.2$, and $\varphi=13\%$ (Couette flow).

$\tilde{\epsilon}=3.2$ taking into account the hydrodynamic forces, which in our situation are of the same order of magnitude as thermal random forces.

Finally, the obtained distributions confirm the existence of polydisperse chaining structures with living times of the order of ms, which are partly broken by an hydrodynamic shear. They also demonstrate that our dynamical experiment is sensitive to very thin structuration at the nanoscale.

In conclusion, through the coupled phenomena of negative viscosity and vortico-magnetic resonance, we give a direct and vivid experimental evidence of the energy conversion between the magnetic and mechanical degrees of freedom of particles. The opportunity to drive the viscosity by a tiny change of ac field frequency may clear the way to new applications such as tunable dampers. Besides, the wide distribution of relaxation time responsible for the sharp magnetic resonance could be related to the existence of short chains in the MF without applying strong magnetic field. A theoretical analysis for chain distribution supports this assumption. So far, the dynamic behavior of chaining dipolar spheres was studied only for particles of microscopic dimensions [18,19]. Thus the experiments presented in this paper open new trends in the dynamic of chaining systems at the nanoscale.

We are indebted to S. Neveu for providing us with the MF sample and to J. Servais and P. Lepert for their technical assistance. We are grateful to A. Cebers and to D. Quemada for fruitful discussions. M.I.S. thanks the Université Paris 6 for providing him a PAST position. J.-C.B. is affiliated with the Université Paris 7.

[1] P. G. de Gennes and P. A. Pincus, Phys. Kondens. Mater. **11**, 189 (1970).
[2] M. E. van Leeuwen and B. Smit, Phys. Rev. Lett. **71**, 3991 (1993).
[3] J. J. Weis and D. Levesque, Phys. Rev. Lett. **71**, 2729 (1993).
[4] M. J. Stevens and G. S. Grest, Phys. Rev. Lett. **72**, 3686 (1994).
[5] R. P. Sear, Phys. Rev. Lett. **76**, 2310 (1996).
[6] M. I. Shliomis, T. P. Lyubimova, and D. V. Lyubimov, Chem. Eng. Commun. **67**, 275 (1988).
[7] R. E. Rosensweig, *Ferrohydrodynamics* (Cambridge University Press, Cambridge, England, 1985).
[8] R. E. Rosensweig, J. Popplewell, and R. J. Johnston, J. Magn. Magn. Mater. **85**, 171 (1990).
[9] A. V. Lebedev and A. F. Pshenichnikov, J. Magn. Magn. Mater. **122**, 227 (1993).
[10] J.-C. Bacri, A. Cebers, and R. Perzynski, Phys. Rev. Lett. **72**, 2705 (1994).
[11] M. I. Shliomis and K. I. Morozov, Phys. Fluids **6**, 2855 (1994).
[12] J.-C. Bacri, R. Perzynski, M. I. Shliomis, and G. I. Burde, Phys. Rev. Lett. **75**, 2128 (1995).
[13] R. E. Rosensweig, Science **271**, 614 (1996).
[14] F. Gazeau, B. M. Heegaard, J.-C. Bacri, A. Cebers, and R. Perzynski, Europhys. Lett. **35**, 609 (1996).
[15] R. Massart, IEEE Trans. Magn. **17**, 1247 (1981).
[16] J.-C. Bacri, F. Boué, V. Cabuil, and R. Perzynski, Colloids Surf. A **80**, 11 (1993).
[17] R. Pynn, J. B. Hayter, and S. W. Charles, Phys. Rev. Lett. **51**, 710 (1983).
[18] G. Helgesen, A. T. Skjeltorp, P. M. Mors, R. Botet, and R. Jullien, Phys. Rev. Lett. **61**, 1736 (1988).
[19] F. L. Calderon, T. Stora, O. M. Monval, P. Poulin, and J. Bibette, Phys. Rev. Lett. **72**, 2959 (1994).
[20] J. Israelachvili, *Intermolecular and Surface Forces* (Academic, London, 1991).
[21] L. D. Landau and E. M. Lifshitz, *Statistical Physics* (Pergamon, New York, 1969).
[22] M. I. Shliomis *et al.* (unpublished).